# OPTIMUM EXCITATION COIL CURRENT PATTERN FOR A DISCRETE COIL INDUCED CURRENT EIT SYSTEM

Adnan KÖKSAL*, B. Murat EYÜBOĐLU**, and Mehmet DEMÝRBÝLEK*

*Hacettepe University, Electrical and Electronics Eng. Dept., 06532 Ankara, TURKEY
**Middle East Technical University, Electrical and Electronics Eng. Dept., 06532 Ankara, TURKEY
E-mail:koksal@hacettepe.edu.tr.

***Abstract-*** Distinguishability of a discrete coil induced current electrical impedance tomography system is analyzed. The solution methodology of the forward problem of this system is explained. An optimization procedure using this forward problem solution is developed to find optimum currents that maximize the distinguishability. For concentric inhomogeneity problem, it is shown that the coil currents can be optimized to focus the current density in any desired location, in the field of view. Optimum coil currents under limited peak coil currents constraint and limited total power constraint are determined. Examples that demonstrate the performance of the system are presented.

***Key Words:*** Electrical Impedance Tomography, Magnetic Impedance Tomography, Distinguishability, Induced Current, Discrete Coil

## I. INTRODUCTION

Electrical Impedance Tomography (EIT) is an imaging technique, first employed in geophysical imaging, later developed as a medical imaging modality within the last twenty years (Boone et al (1997), Rigaud and Morucci (1996)). In EIT, images of the absolute conductivity distribution or variations in conductivity distribution are reconstructed, based on electrical measurements performed on the surface of the conducting region. In the case of injected current EIT, current is injected through 16-32 electrodes and measurement of voltage along the boundary of the object are used to reconstruct the conductivity image. Induced current EIT (Scaife et al (1990), Purvis et al (1993), Healey et al (1993), Freeston and Tozer (1995), Gençer (1993), Gençer and Ýder (1994), Gençer et al (1996)) works with similar principles, the main difference being the induction of the current using a coil(s) located outside the object. Seagar (1983), Seagar and Bates (1984), and Seagar et al (1987) analyzed the systems' sensitivity required for detection of a given inhomogeneity for a single drive injected current EIT. A similar study was performed by Anderson et al (1995) for the continuous coil induced current EIT systems. Distinguishability of an EIT system is defined by Isaacson (1986) as the system's ability to detect conductivity difference of an inhomogeneity from the background. How well the system is able to do so is mathematically expressed as the norm of the difference of potential at the boundary for the cases where the inhomogeneity is and is not present. Current patterns that maximize the distinguishability of a concentric inhomogeneity are studied in under several constraints for the injected current EIT (Isaacson (1986), Cheney and Isaacson (1992)). Later, the effect of constraints on the distinguishability performance of the system is studied in (Eyüboğlu and Pilkington (1993)), where it is shown that while cosine drive is better under constant power constraint, opposite drive has a better distinguishability when the total current injected to the object is kept constant. Opposite drive has been shown to be actually the best under constant injected current constraint using an optimization procedure (Köksal and Eyüboğlu (1995)).

The scope of this paper is to extend the distinguishability concept defined by Isaacson (1986) for concentric objects in injected current EIT systems to discrete coil induced current EIT systems. Another goal is to obtain optimum coil currents under different constraints on coil currents. Section 2 summarizes the distinguishability analysis and optimization method. Section 3 gives some examples of forward analysis and of distinguishability optimization under two different constraints. Conclusions and future work are given in Section 4.

## II. METHOD OF ANALYSIS

In EIT, independent measurements are obtained by changing the positions of the current injection electrodes or by changing the location of the coil. In the case of injected current EIT, an optimum current density may be created by injecting varying amounts of current through several pairs of electrodes (Isaacson (1986), Cheney and Isaacson (1992)). With a similar approach, induced current in the object can be controlled efficiently using the discrete coil configuration having fixed location as shown in Fig. 1 and by changing the individual coil currents.

The problem shown in Fig.1 can be solved easily using quasi-static assumption and by neglecting the displacement field in the object. Typical operating frequencies of EIT systems and the nature of conductivity distributions in living bodies in this frequency range justifies this assumption. A detailed formulation of the solution for a single coil case is given in (Gençer (1993)). The concentric inhomogeneity problem can be solved analytically using a quasi-static approximation. According to this approximation, coil currents produce a magnetic field which induces an electric field in the object, however, the contribution of this induced electric field to the total magnetic field is negligible. The second approximation used is both related to the frequency of operation and electrical properties of the object and of inhomogeneity. In the frequency regime of EIT, dielectric properties of objects are much less important than their conductor properties ($\sigma >> \omega\varepsilon$), and hence the displacement currents are neglected.

If one calculates the magnetic vector potential, A, for the coil excitation, under the given assumptions, the solution for potential $\Phi$ is readily expressed in terms of the Fourier coefficients of $A_n$. Calculation of $A_n(R_i(\theta))$ for any angular section of discrete coils is carried out using numerical integration and the calculation for the segments extending to infinity is carried out analytically. Thus in the solution of the forward problem, first $A_n$ is calculated at the boundaries of the problem and its truncated Fourier series with desired accuracy (less than 1% error) is found. The Fourier coefficients $C_m$, $D_m$, $E_m$, $F_m$ of $A_n$ at the two boundaries are sufficient to determine the solution of the forward problem.

For the distinguishability analysis, consider the problem shown in Fig.1 and choose $\sigma_2=1$, $R_2=1$, and $\sigma_1=\sigma$, $R_1=R$. Let $V_2(\theta)$ and $V_1(\theta)$ denote the solutions for potential at the outer boundary $R_2=1$ for the cases where the inhomogeneity is and is not present, respectively. $L_2$ norm of the difference between the voltages $V_2(\theta)$ and $V_1(\theta)$, denoted by $\|V_d(\theta)\|$, is the distinguishability measure defined by Isaacson (1986). The distinguishability function is obtained in terms of aforementioned potential solutions and Fourier coefficients of $A_n$ as:

$$V_2(q) - V_1(q) = \sum_{m=1}^{\infty} \frac{-2mR^{m+1}}{1+mR^{2m}} \left\{ \left[ R^{m-1} C_m - E_m \right] \cos mq + \left[ R^{m-1} D_m - F_m \right] \sin mq \right\}$$

When this potential difference is larger than the measurement precision, the inhomogenity causing that difference is distinguishable. This defines the theoretical limit under a finite measurement precision and there are several other limitations due to reconstruction of the images from the measured data. An object may be distiguishable based on the criteria used in this work may not be identifiable in the reconstructed image.

Optimum (or best) currents are those which maximize the distinguishability measure defined earlier. The solution of this problem is in a form similar to the solution of the forward problem, but here the unknowns are the coil currents. An optimization procedure for the currents is developed to optimize $\|V_d(\theta)\|$ under two different constraints. In the first constraint, the coil current amplitudes are confined in an interval, i.e. $|I_j| \leq 1$. This is equivalent to limiting the maximum current density in the object. In the second constraint, $L_2$ norm of the coil currents vector is chosen as unity, i.e. norm(I)=1. This is equivalent to keeping the power supplied by the coils constant.

The optimization problem is solved by defining every parameter related in matrix form. The forward problem solution is obtained in the same manner, the main difference being is that the currents are known in the forward problem. The modular structure of the analysis method enables to use the same analysis data for different coil currents.

## III. RESULTS

The six coil system of Figure 1 is used for the examples given and concentric inhomogeneity case is investigated. Operating frequency of the system is assumed as f=50 kHz. In all the cases investigated, it is found that five Fourier coefficients are sufficient to represent the normal components of the magnetic vector potential at both boundaries of the inhomogeneity, with less than 1% $L_2$ norm error.

As a first example, $R_1=0.5$, $R_2=1$, $R_3=2$, $\sigma_1=10$ and $\sigma_2=1$ are chosen. This corresponds to an inhomogeneity which is a good conductor. Figure 2 shows the resulting current distribution in the object when the optimal currents obtained after the optimization are applied. These optimum currents are obtained under norm(I)=1 constraint, and are I=[0.41 0.56 0.15 -0.41 -0.56 -0.15]. Resulting $\|V_d\|$ value in this example is 0.37 mV. The optimum (best) coil excitation results in a current density distribution which is localized on the conductor inhomogeneity as can be seen from Figure 2. Also the best current pattern resembles a sinusoid which is in accord with the earlier result obtained by the authors and others using constant power constraint in injected current EIT.

The same problem described above is solved using $|I_j| \leq 1$ constraint to see the effect of the constraints on the solution. Optimum coil currents in this case are obtained as I=[1 1 1 -1 -1 -1] which is simply equivalent of opposite drive in injected current EIT. This result is also in agreement with the earlier results. The current distribution in the object when optimum coil currents are applied are shown in Figure 3. Resulting $\|V_d\|$ in this example is 0.86 mV.

As a second example, a problem having the same geometry as the first problem is chosen but this time the inhomogeneity is made an insulator, i.e. $\sigma_1=0$. Optimum currents under norm(I)=1 constraint are I=[0.41 0.56 0.15 -0.41 -0.56 -0.15], which is the same as the conductor case. Figure 4 shows the current distribution in the object. As expected, again the same cosine pattern is obtained for the insulator case. Optimum currents for the second constraint is the opposite drive as the first example, and the results and interpretation is very similar.

$\|V_d\|$ values given above for the examples cannot be compared directly because optimum currents for different constraints have neither the same peak value nor the same norm. In order to compare different drive patterns fairly, an approach of Cheney and Isaacson (1992) is followed and three currents are calculated as, $I_1$=[ -1.00 1.00 1.00 1.00 -1.00 -1.00], $I_2$ =[ 0.73 1.00 0.27 -0.73 -1.00 -0.27 ] , and $I_3$ = [ 1.00 1.37 0.37 -1.00 -1.36 -0.37]. Here, $I_1$ and $I_2$ have the same peak value of 1 and norm of $I_3$ is equal to that of $I_1$. $I_2$ and $I_3$ are obtained from optimum current for constant power case (cosine drive) by proper scaling. To compare these currents, minimum detectable object radius for the three currents are calculated as a function of the inhomogeneity conductivity, assuming a measurement noise of

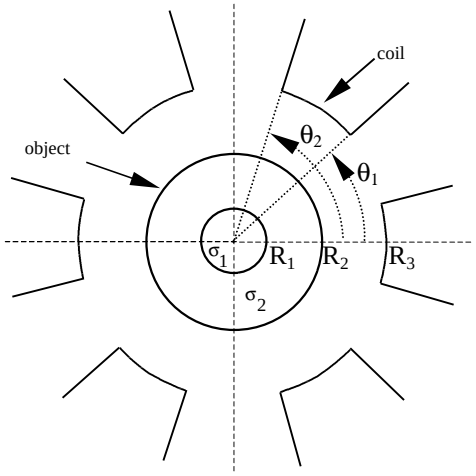


Figure 1

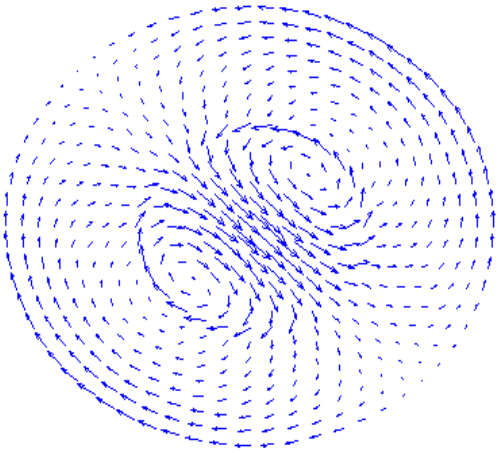

Figure 2

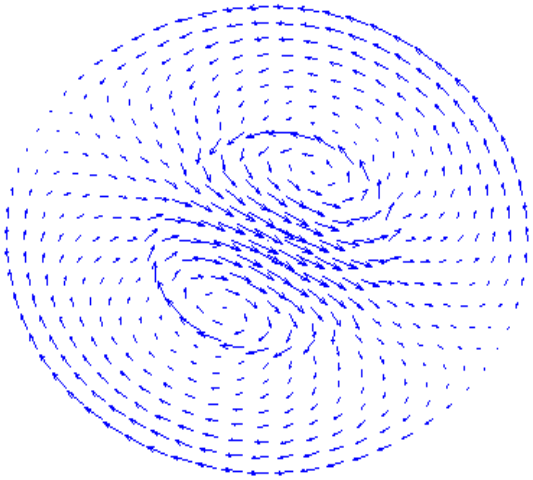

Figure 3

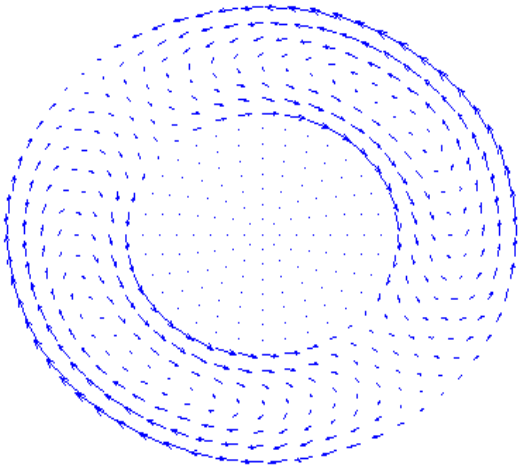

Figure 4

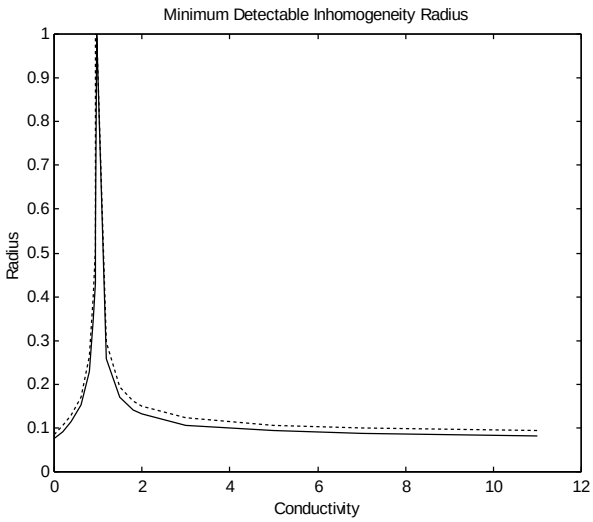


Figure 5

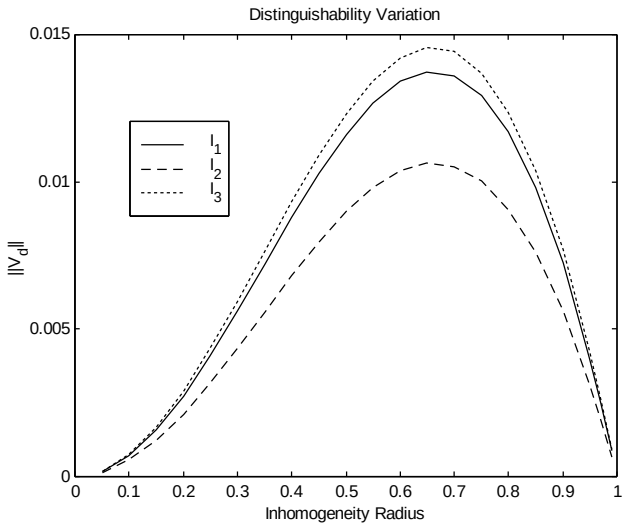


Figure 6

0.5mV. The background conductivity is taken as $\sigma_2$=1. Figure 5 shows the comparison of minimum detectable object radii for $I_1$ and $I_2$. It is found from this comparison that, when the peak current value is the same, opposite drive is better than cosine drive in terms of distinguishability. On the other hand, when total power is kept constant, cosine drive is slightly better than the opposite. For a measurement noise of 0.5mV and $R_2$=1, $R_3$=2, $\sigma_2$=1, the values of minimum detectable object radius (in cm) are also listed in Table 1 for easy numerical comparison of the three cases.

Table 1: Minimum detectable object radii (minimum $R_1$), for $I_1$, $I_2$, and $I_3$

| $\sigma$ | 0 | 0.2 | 0.4 | 0.6 | 0.8 | 0.9 | 0.93 | 0.94 | 0.97 | 1.2 | 1.8 | 2 | 5 | 9 |
|---|---|---|---|---|---|---|---|---|---|---|---|---|---|---|
| $R_{min1}$ | 7.5 | 9.1 | 11.4 | 15.1 | 22.9 | 34.5 | 43.1 | 47.7 | 99.9 | 25.7 | 14.2 | 13.2 | 9.3 | 8.5 |
| $R_{min2}$ | 8.5 | 10.4 | 12.9 | 17.1 | 26.3 | 39.9 | 51.1 | 58.3 | 99.9 | 29.6 | 16.1 | 14.9 | 10.4 | 9.7 |
| $R_{min3}$ | 7.3 | 8.9 | 11.2 | 14.5 | 22.2 | 33.3 | 41.5 | 46.0 | 99.9 | 24.9 | 13.8 | 12.8 | 8.9 | 8.1 |

Figure 6 shows calculated $||V_d||$ values as a function of inhomogeneity radius for a fixed inhomogeneity conductivity of 10. In this figure, $||V_d|_{max}$ occurs between R=0.6 and R=0.7 and decreases to zero for all three currents at R=1. The reason of this behaviour is the quasi-static operation of induced current EIT system. The effect of magnetic field at the two boundaries cancel each other as the two boundaries get close.

## IV. CONCLUSION

In this work, distinguishability of a discrete coil induced current EIT system for a concentric inhomogeneity is analyzed. The purpose of the proposed discrete coil configuration was to control the current distribution inside the object without moving coils, or the object under investigation. It was shown through examples that this has been successfully achieved. The currents that maximize the distinguishability are obtained for two different constraints: Limited peak coil current and constant total supplied power. It has been found that, for concentric inhomogeneity, cosine drive is best for constant total power constraint and opposite drive is better for limited peak coil current case.

Further research will focus on obtaining the optimum currents for eccentric inhomogeneities and on determining minimum detectable object radius for that case. Optimizing the size of the coils and the number of coils to be used is also subject to further investigation. An adaptive algorithm may be developed to obtain the best current pattern which maximizes the distinguishability for an unknown conductivity distribution, utilizing successive excitations and potential measurements.

## REFERENCES


**Anderson D K, Tozer R C and Freeston I L**, Analytic solution of the forward problem for induced current impedance tomography systems, *IEE Proc. A Sci. Meas. Technol*., vol.142, pp.415-432, 1995.

**Boone K, Barber D, Brown B**, Review imaging with electricity: Report of the European Concerted Action on Impedance Tomography, *Journal of Medical Engineering and Technology*, vol.21, pp.201-232, 1997.

**Cheney M, Isaacson D**, Distinguishability in impedance imaging, *IEEE Trans. on Biomed. Eng*., vol.BME-39, pp.852-860, 1992.

**Eyüboğlu B M, Pilkington T C**, Comments on distinguishability in electrical impedance imaging, *IEEE Trans. on Biomed. Eng.*, vol.BME-40, pp.1328-1330, 1993 (corrections in *IEEE Trans. on Biomed. Eng.*, BME-41, p.505, 1994).

**Freeston I L, Tozer R C**, Impedance imaging using induced currents, *Physiological Measurement*, vol.16, supp3A, pp.257-266, 1995.

**Gençer N G**, Electrical impedance tomography using induced currents, Ph.D. Thesis, Middle East Technical University, 1993.

**Gençer N G, Ýder Y Z**, A comparative study of several exciting magnetic fields for induced current EIT, *Physiological Measurement*, vol.15, supp.2A, pp.51-57, 1994.

**Gençer N G, Ýder Y Z, Willamson S J**, Electrical Impedance Tomography: Induced-current imaging achieved with a multiple coil system, *IEEE Trans. Biomed. Eng*, vol.43(2), pp.139-149, 1996.

**Healey T J, Tozer R C, Freeston I L**, Impedance imaging of 3D objects using magnetically induced currents, *14th Ann. Int. IEEE-EMBS Conf. Proc.*, pp.1719, 1993.

**Isaacson D**, Distinguishability of conductivities by electric current computed tomography, *IEEE Trans. Med. Imaging*, vol.5, pp.91-95, 1986.

**Köksal A, Eyüboğlu B M**, Determination of optimum injected current patterns in electrical impedance tomography, *Physiological Measurement*, vol.16, supp3A, pp.99-109, 1995.

**Rigaud B, Morucci J P**, Bioelectrical impedance techniques in medicine part III: Impedance imaging first section: General concepts and hardware, *Critical Reviews in Biomedical Engineering*, vol.24, No:4-6, pp.467-597, 1996.

**Purvis W R, Tozer R C, Anderson D K and Freeston I L**, Induced current impedance imaging, *IEE Proceed. A Sci. Meas. Techl*., vol.140, pp.135-141, 1993.

**Seagar A D**, Probing with low frequency electric currents, PhD Thesis, University of Canterbury, Christchurch, New Zealand , 1983.

**Seagar A D, Bates R H T**, Full wave computed tomography Part 2: Resolution limits, *IEE Proceedings A*, vol.131, No:8, pp.616-622, 1984.

**Seagar A D, Barber D C and Brown B H**, Theoretical limits to sensitivity and resolution in impedance imaging, *Clin. Phys. Physiol. Meas.*, vol.8, Supp.A, pp.13-31, 1987.

**Scaife J M, Tozer R C, Freeston I L**, Real and imaginary impedance images using induced currents, *Ann. Int. IEEE-EMBS Conf. Proc.*, vol.12, No.1, pp.116-17, 1990.